IEEE Access
Multidisciplinary | Rapid Review | Open Access Journal

Received February 2, 2019, accepted March 17, 2019, date of publication March 25, 2019, date of current version April 9, 2019.

Digital Object Identifier 10.1109/ACCESS.2019.2907114

A New Gabor Filter-Based Method for Automatic Recognition of Hatched Residential Areas

JIANHUA WU[1,2], PENGJIE WEI[2], XIAOFANG YUAN[2], ZHIGANG SHU[3], YAO-YI CHIANG[4], ZHONGLIANG FU[5], AND MIN DENG[1]

[1]School of Geosciences and Info-Physics, Central South University, Changsha 410012, China
[2]School of Geography and Environment, Jiangxi Normal University, Nanchang 330022, China
[3]Bureau of Land and Resource of Jing'an County in Jiangxi Province, Yichun 330600, China
[4]Spatial Sciences Institute, University of Southern California, Los Angeles, CA 90089-0374, USA
[5]School of Remote Sensing and Information Engineering, Wuhan University, Wuhan 430079, China

Corresponding authors: Jianhua Wu (wjhgis@126.com) and Pengjie Wei (wipjie@126.com)

This work was supported in part by the National Natural Science Foundation of China (NSFC) Projects under Grant 41201409, Grant 41561084, and Grant 41661083, in part by the scholarship from the China Scholarship Council (CSC) under Grant 201409470010, in part by the China Postdoctoral Science Foundation under Grant 2018M632991, and in part by the Open Foundation of Key Laboratory for National Geography State Monitoring (National Administration of Surveying, Mapping and Geoinformation) under Project 2016NGCM01 and Project 2016NGCM07.

ABSTRACT Extracting residential areas from historical raster topographic maps benefits to analyze land type change. The existing algorithms have the shortcomings including easily misidentifying objects and low positional accuracy of the identified boundary, so we have presented a new automatic recognition method based on Gabor filter for extracting residential areas from historical raster topographic maps. First, the method detected the hatched areas using Gabor filter, Gaussian smoothing, binarization, erosion, and an operation. Afterward, an endpoint of a hatched line on the top of the hatched areas was taken as the starting point, then tracing a boundary point of the residential area along a hatched line toward northeast 45 degrees direction using dynamic filling strategy. Second, an adjacent boundary point was traced according to the pixel value relation of eight neighborhoods by taking the first found boundary point as a starting point. In the tracking process, removing the noises using the pixel value relation of the neighboring pixels and the designed strip detector. Ultimately, the residential boundary was obtained. The experiments were carried out on the samples of three typical areas. The results showed that our method was effective and practical, and outperformed the previous methods in integrity and positional accuracy of the residential boundary.

INDEX TERMS Residential areas recognition, raster map, Gabor filter, data mining, image processing.

I. INTRODUCTION

Currently, many departments of surveying and mapping geographic information have stored a large number of digital raster maps containing rich and valuable geographic information such as residential area, topography, vegetation, road names and so on. Historical maps are unique sources of retrospective geographical information [1]. Geographic information extracted from historical raster maps can support a wide range of applications and research areas, for example, land cover change and biogeography research [2]. However, these implicit geographic information of raster maps are difficult to be used for GIS spatial analysis due to inferior graphic quality and great complexity of maps.

The associate editor coordinating the review of this manuscript and approving it for publication was Jiachen Yang.

Figure 1a is an archived historical raster map published in 1924 by the director general at the ordnance survey office, Southampton. Its map scale is six inches to one statute mile. Figure 1b is the remote sensing image obtained from Google Maps covering the same area of Figure 1a. By manually comparing Figure 1a and Figure 1b, it is easy to find that most of the buildings, vegetation and other features have changed except the St Nicholas Church (Figure 1c). But it is difficult for a computer to recognize these changes. Generally it is needed to vectorize the historical raster map and overlay the vectorization layers with an up-to-date vector topographic map for land change analysis. If only a few raster maps are needed for data analysis, the manual map vectorization method may be adopted, however, this approach is subjective and time-consuming. If a lot of raster maps are needed for

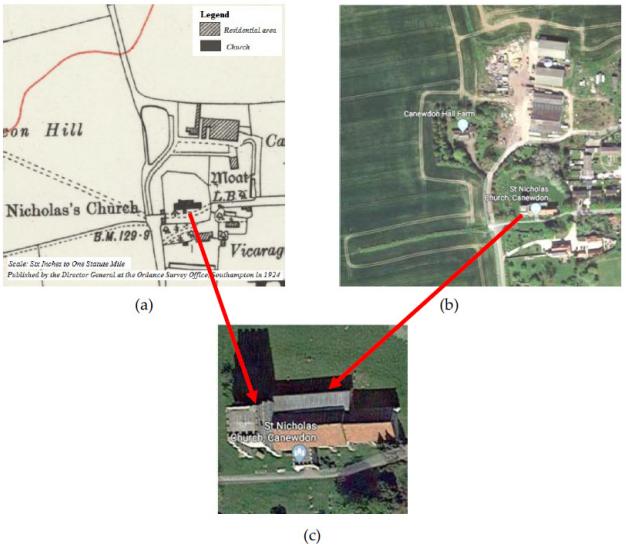

FIGURE 1. Example of land cover change around Canewdon Hall Farm: (a) Raster map published in 1924 (https://maps.nls.uk/view/101457131), (b) Remote sensing image (http://www.google.cn/maps/@51.6179934,0.7389461,318m/data=!3m1!1e3?hl=en, Imagery @2018 DigitalGlobe, Getmapping plc, Infoterra Ltd& Bluesky, The GeoInformation group, map data @2018 Google), (c) Location of St Nicholas Church.

vectorization or multiple departments need to vectorize the map covering the same geographic area, it is necessary to design auto-recognition algorithms for extracting geographic information from raster maps to avoid or greatly reduce the work of artificial vectorization.

Residential area is one of the most important elements of the topographic map. In 1:10000 or 1:50000 historical raster topographic map, the residential area was usually represented by the symbol with hatched 45 degree lines. These residential areas are scattered, no fixed size and shape, and often connect with other map symbols (Figure 1a), besides the poor image quality, which make the automatic identification of such residential areas facing huge challenges. In view of the fact that the existing methods are prone to appear recognition errors, the accuracy of recognition boundary positions is not high and the practicality is poor. To solve this problem, this paper presents a new method for automatic identification of hatched residential areas with hatched 45 degree lines in the raster map. The proposed method adopts the advantage of Gabor filter for recognizing periodic texture to recognize hatched areas, and presents dynamic filling strategy to detect the tracking starting point of boundary, according to the pixel value relationship of neighborhood pixels and the designed bar detector to eliminate noise. It not only more accurately identifies the hatched residential areas, but also greatly reduces processing time by comparing with manual map vectorization. The significance of our work lies mainly in two sides: It is helpful to realize the automatic vectorization of the residential areas in the historical maps and the identified residential areas are helpful to analyze the change of land type.

II. RELATED WORK

Information extraction from raster map has been receiving attention of scholars, for example, extracting contour lines [3], road intersections [4], forest areas [5] and human settlements [6], [20]. As early as a decade ago, in order to realize the vectorization of raster maps, many scholars carried out the study of map object recognition [6]–[12], but few studies have been done in this area in recent years. Liu Xue et al. proposed an integrated approach for segmentation and identification of housing objects in 1998 [6]. This method used the direction and the spatial interval of the hatched line to obtain the hatched area, but the identified residential area was still stuck to other objects and the shape accuracy of housing was obviously not high. Hao Xiangyang et al. proposed a four-directional RLS (Run-length Smearing) method for image segmentation in terms of the structural features of hatched-polygons [7]. All polygons with hatched line were segmented into black block through four-directional transformation, after many times of treatment including contraction transformation, disconnection of adhesions (adhesion is a symbol object like a road or another object connecting with the polygon with hatched line), re-expansion transformation and refinement. This method was easy to mistakenly identify annotations as the hatched residential areas. The identified boundary of polygons were incomplete and the position precision was uncertain. Chen Yang et al. proposed the method of using Gabor filter to detect the internal hatched line of residential area in the refined and pruned raster map [12]. This method can easily lead to the accuracy loss of the boundary position, and the boundary tracking process will stop when it encounters the sign of adhesion. So a connection processing of disconnect outlines is needed in post-processing, but whether to successfully connect the adjacent endpoints of fracture or not depends on a manual search buffer. Regine Brügelmann constructed a vector template to detect the hatched texture. The vector template consists of the travel length of the black and white pixels in the horizontal direction in the hatched region [9]. The result of literature [9] also has the deficiencies of large accuracy loss of boundary position and adhesions. It is easy to find all the above methods can not directly output raster or vector data with closed boundaries of residential areas. In general, there are still some deficiencies in the existing methods of raster map object recognition. In recent years, some scholars proposed machine learning-based methods for effectively detecting the buildings from high resolution aerial images [18], [19], while those methods require a large amount of sample data and long time for data training. J.H. Uhl et al. adopted the method using context-based machine learning for extracting human settlement footprint from historical topographic map [20]. While they used the contemporary building data for collecting graphic examples and the objects to be recognized were the color-filled buildings.

In contrast to the previous researches on residential area identification [7], [9], [12], our approach improves the boundary position accuracy and boundary integrity, and it has

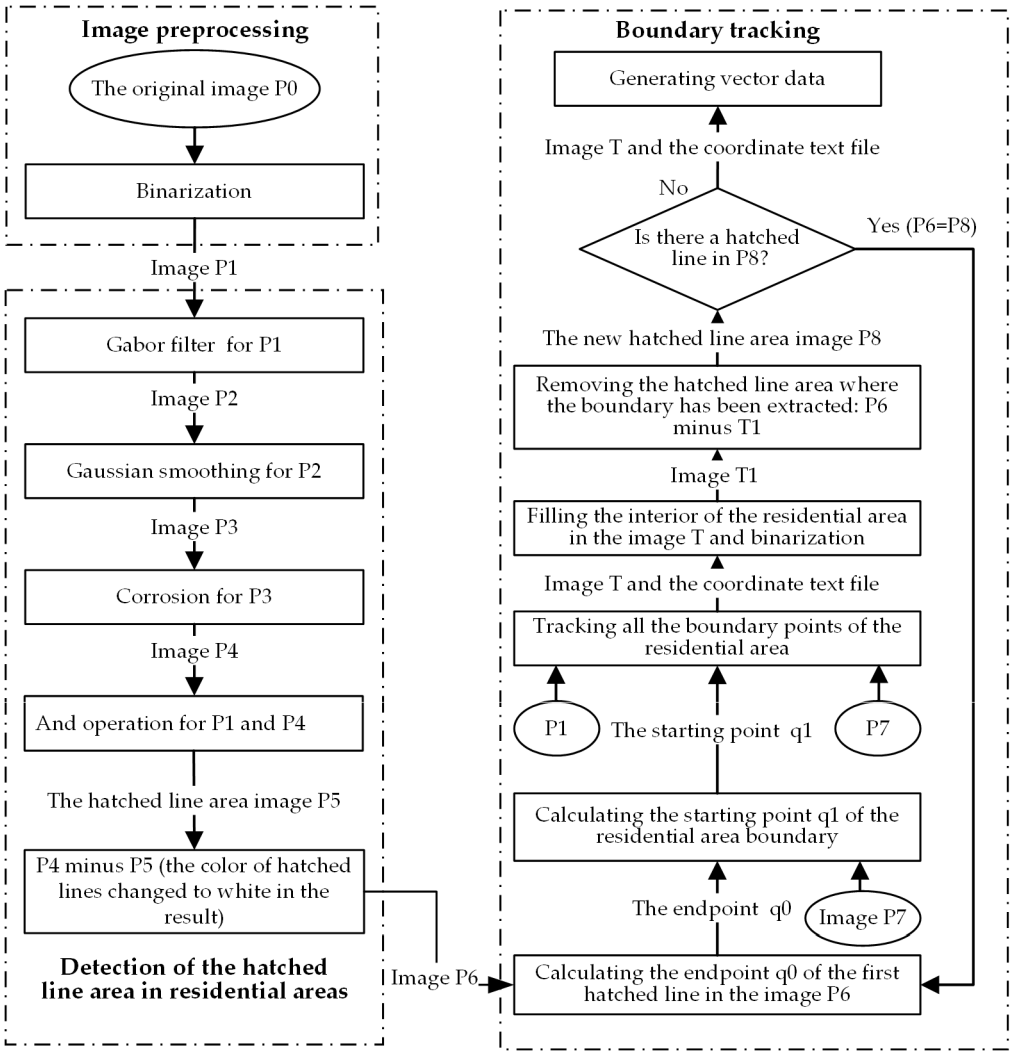

FIGURE 2. Identification and vectorization of residential areas.

advantages of strong anti-noise ability (it can effectively identify and remove adhesions) and high degree of automation.

III. RESIDENTIAL AREA AUTOMATIC RECOGNITION ALGORITHM

A. RESIDENTIAL AREA IDENTIFICATION PROCESS

There are three main steps for automatically identifying residential areas from a color or grayscale raster maps. The first step is binarization processing of the raster map image. The second step is to detect and extract the hatched lines of the residential area. The third step is to track the residential boundary. The specific procedures and steps shown in Figure 2. Where image P7 is a backup image of the original image P1, image P1 will be changed during boundary tracking, image T only records the boundary points of residential areas by drawing pixels and the coordinate text file records the coordinate values of all the boundary points. The time complexity of the residential area identification algorithm is O (n^3).

B. GABOR FILTER

The internal hatched lines of residential area appear a kind of periodic texture structure. To solve the problem of locating residential areas in the raster map image, we adopted the two-dimensional Gabor kernel function as a Gabor filter that is suitable for texture expression to find the position of residential area. To solve the problem that the Fourier transform does not have locality, Dennis Gabor took the window function of the Short Time Fourier Transform (STFT) as Gaussian function in 1946 and proposed the Gabor transform [14]. Gabor transform is the optimal STFT, which can provide both localized information in time domain and frequency domain. The two-dimensional Gabor filter was first proposed by Daugman in 1985 [15]. The Gabor filter is a band-pass filter with frequency and directional selectivity [17], which has excellent spatial localization and direction selectivity, and can acquire the spatial frequency of multiple directions and local structural features in the local area of image [16]. It can be regarded as the product of a Gaussian function and a

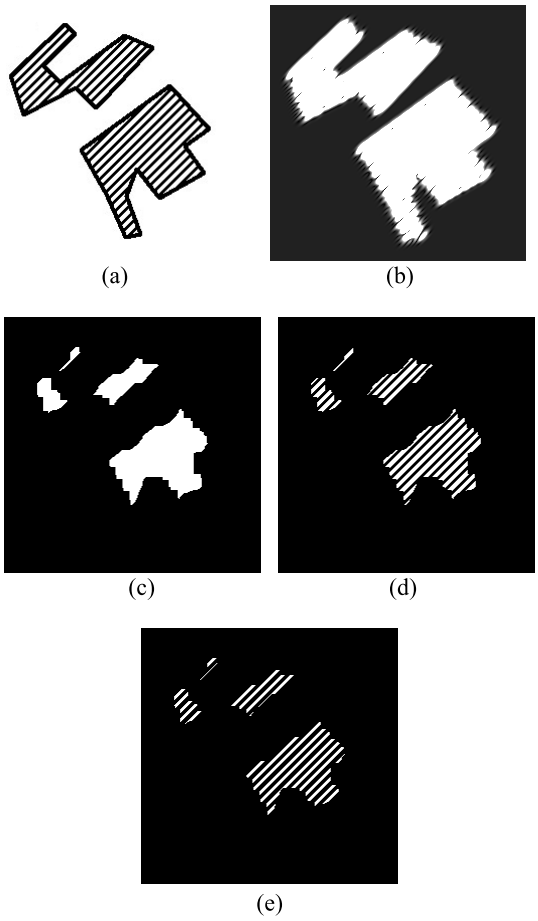

FIGURE 3. The schematic diagram of detecting hatched line: (a) the binary image, (b) the filtered image, (c) the filtered image is successively processed by Gaussian smoothing, binarization and erosion, (d) the clipped hatched lines, (e) the extracted hatched lines expressed in white.

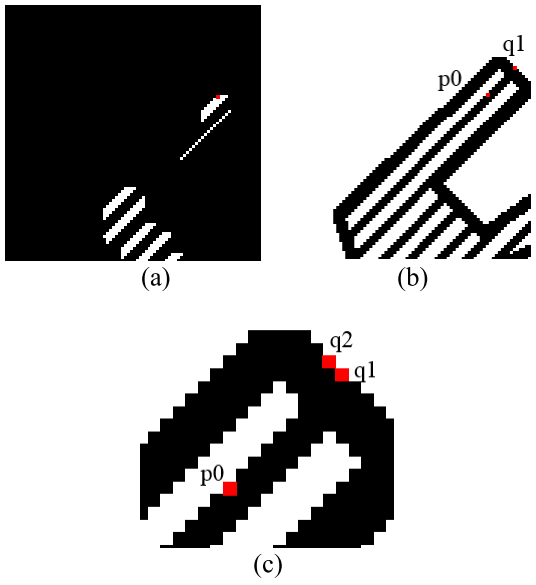

FIGURE 4. Several key points for tracking boundary: (a) the location (/coordinate) of the first white pixel denoted by red point, (b) p0 and q1, (c) partial figure of (b) showing the traced connection point p2.

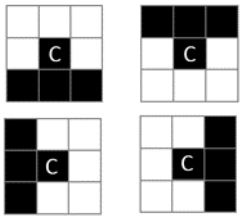

FIGURE 5. Single pixel noise on boundary.

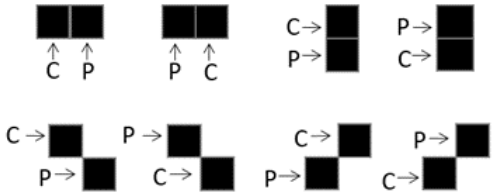

FIGURE 6. Spatial position relationships between two adjacent points.

sine plane wave [17]. The two-dimensional Gabor transform belongs to the windowed Fourier transform, which essence is to conduct two-dimensional convolution using Gabor kernel function for the image. The mathematical expression of two-dimensional Gabor kernel function is shown in formula (1 − 3) [17].

$$g(x, y; \lambda, \theta, \phi, \sigma, \gamma) = \exp\left(i\left(2\pi\frac{x'}{\lambda} + \phi\right)\right) \tag{1}$$

The real part is expressed in formula (2)

$$g(x, y; \lambda, \theta, \phi, \sigma, \gamma)_{real} = \exp\left(-\frac{x'^2 + \gamma^2 y'^2}{2\sigma^2}\right)\cos\left(2\pi\frac{x'}{\lambda} + \phi\right) \tag{2}$$

The imaginary part is expressed in formula (3)

$$g(x, y; \lambda, \theta, \phi, \sigma, \gamma)_{image} = \exp\left(-\frac{x'^2 + \gamma^2 y'^2}{2\sigma^2}\right)\sin\left(2\pi\frac{x'}{\lambda} + \phi\right) \tag{3}$$

where $x' = x\cos\theta + y\sin\theta, y' = -xsin\theta + y\cos\theta$, λ represents the wavelength of the sine plane wave in the Gabor kernel function (the frequency of the sine plane wave is f= $1/\lambda$). The valid value should be greater than 2 pixels. θ indicates the direction of Gabor filter (it corresponds to the direction of the internal hatched line in the residential area), and it has a range of 0 to 360 degrees. σ represents the standard deviation of the Gaussian function of the Gabor kernel along the directions of the coordinate axes x and y (the Gaussian function is a normal distribution function, the smaller σ is the more values concentrate the distribution around the expected value, and the larger σ is the more dispersed the value distribution). In general, we think that the standard deviations in the x and y directions are equal. The parameter σ determines the size of the area that Gabor filter kernel can accept and can't be directly assigned, and its value

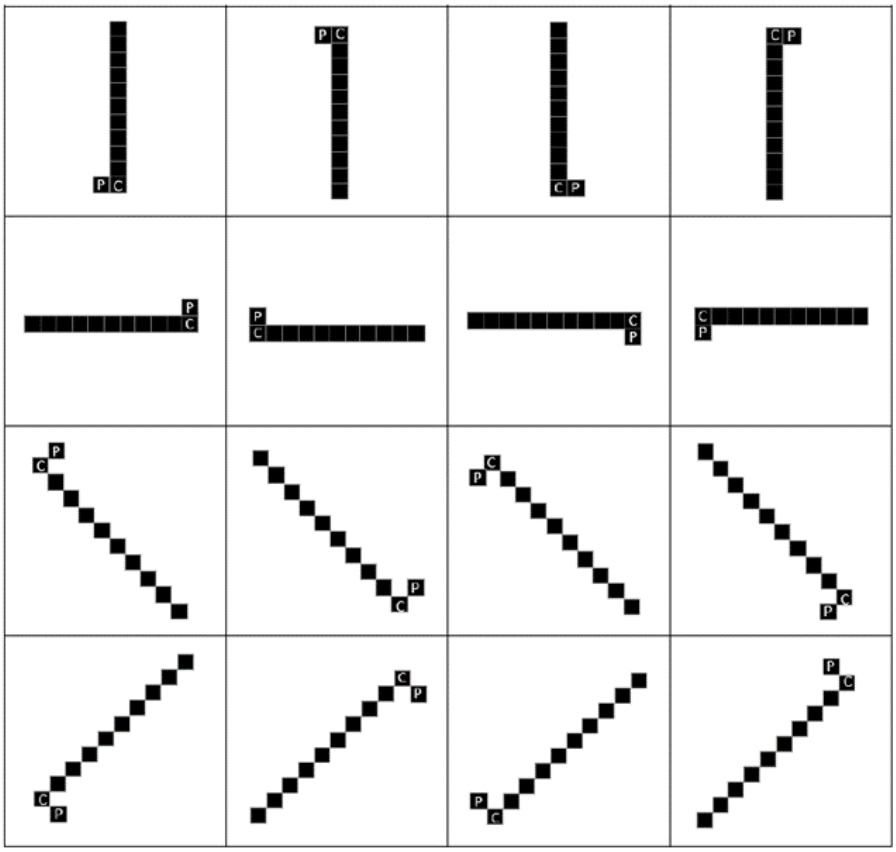

FIGURE 7. Strip detectors with different directions.

is related to b (Bandwidth, that is, the difference between high and low frequency) and λ. The relationship between the above three parameters is shown in formula (4) [12].

$$\frac{\sigma}{\lambda} = \frac{1}{\pi}\sqrt{\frac{ln2}{2}} \cdot \frac{2^b + 1}{2^b - 1} \tag{4}$$

γ in formula (3) represents the spatial aspect ratio that indicates the ellipticity of the Gabor filter and determines the shape of the Gabor function. φ represents the phase offset, its value range is -180 degrees to 180 degrees.

C. DETECTION OF HATCHED LINE USING GABOR FILTER

We utilize the two-dimensional Gabor kernel function as a Gabor filter to filter the raster map image so as to preliminarily find the position of residential areas. To output the hatched area of residential areas as much as possible, this paper also uses Gaussian smoothing, erosion, image and-operation and subtraction-operation to detect the internal hatched line of the residential area. The process of detecting hatched line in residential area is as follows (Figure 3 illustrated this process):

(1) Using Gabor filter to filter the binary image (Figure 3a is the original binary image). The hatched area is obtained after filtering image (Figure 3b), but there are still some disadvantages of the hatched area image (e.g., noise).

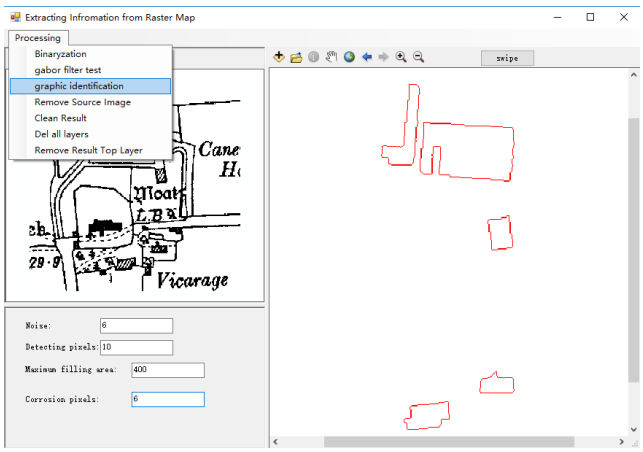

FIGURE 8. Experimental platform.

(2) The filtered image is successively processed by Gaussian smoothing, binarization and erosion. Since the image boundary of hatched area after filtering is rough and fuzzy, the area of the hatched area is slightly larger than that the boundary of the original residential area, and there is noise in the hatched area image (see the Figure 3b). Therefore, Gaussian smoothing, binarization and erosion are required for

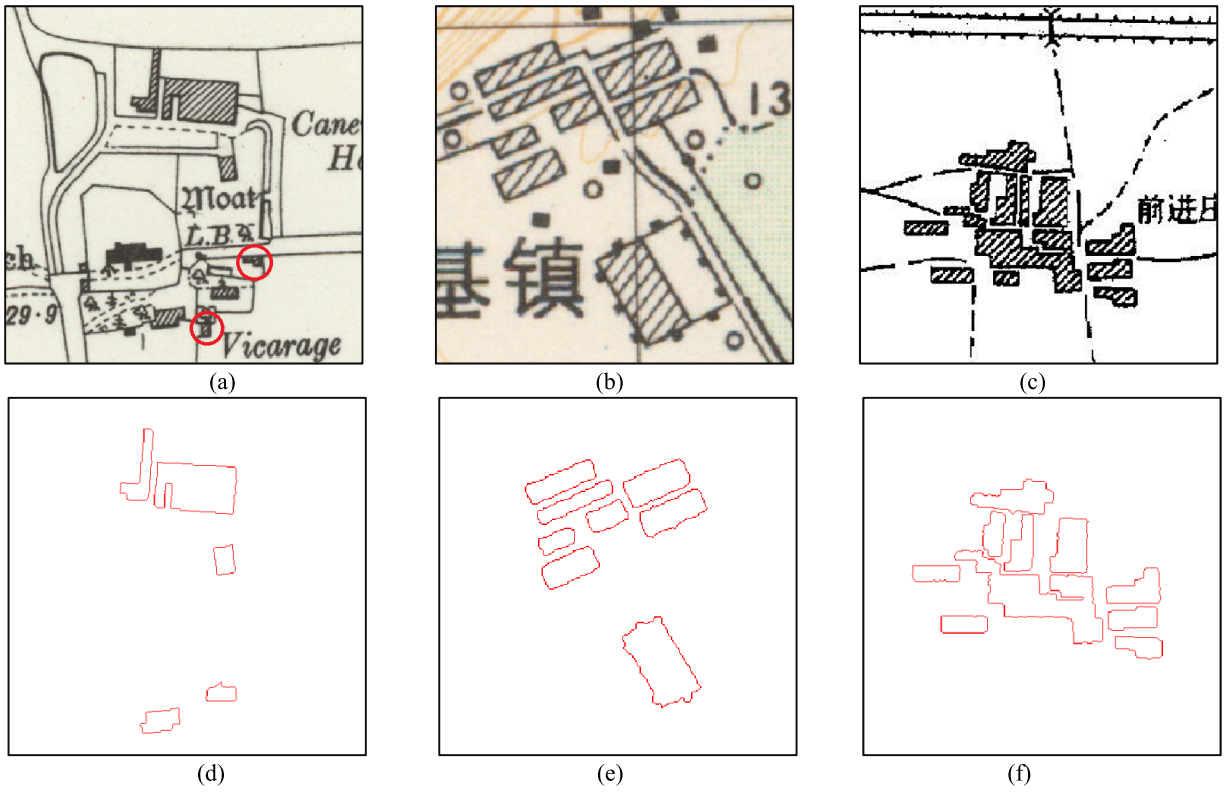

FIGURE 9. Experimental data: (a) map 1, (b) map 2, (c) map 3, (d) the identification result of map1, (e) the identification result of map2, (f) the identification result of map3.

the image to correctly extract the starting point for boundary tracking. The image processing result of this step is shown in Figure 3c.

(3) The hatched line extraction. In order to get the internal hatched line image of residential area, our algorithm needs to do the following. Firstly, performing the and-operation between the image after smooth and erosion and the original binary image to obtain the hatched line image. Then, using the binary image (Figure 3a) and the filtered image after smooth and erosion (Figure 3c) to do and-operation. The result is Figure 3d. After Figure 3c subtracted Figure 3d, we can get the hatched line image where the hatched lines are expressed in white and the interval areas of the hatched lines are expressed in black (Figure 3e).

D. EXTRACTION OF RESIDENTIAL AREA BOUNDARY

The basic idea of the algorithm for extracting residential area boundary is as follows. Firstly, it extracts the endpoints of the hatched line: scanning the pixel of the hatched image line by line to find out the location (/coordinate) of the first white pixel (it is one of the pixels of the endpoint of the hatched line). Taking the images in Figure 3 for example, the location of the first white pixel is the location of red point in the Figure 4a (a partial figure of Figure 3e).

Then it detects the starting point of boundary tracking: to find pixel p0 (see Figure 4b) with the same location of the endpoint (the scanned first white pixel) of hatched line on the original binary image. Taking p0 as the starting point pixel, considering the directions of the hatched lines are basically 45 degrees, and in general, there are no other adhesions in the crossings between the hatched lines and the residential area boundary. So we can get the first residential area boundary point q1 (see Figure 4b) by tracking pixels along the northeast 45 degrees direction of the hatched line. Secondly, it carries on the boundary point tracking. First, we take the boundary point pixel q1 as the starting point to find the pixel q2 (see Figure 4c) that connects q1 by judging the relationships of the eight neighborhood pixel values. Then we take q2 as the starting point to find the next boundary point (not including the boundary point that has been found) connecting to q2 by judging the relationships of the eight neighborhood pixel values. In the process of boundary tracking, our algorithm uses the relationships of neighborhood pixel values and the designed strip detector (see section 3.4.2) to remove the noises. By that analogy, the algorithm continuously tracks the next connection point until the connection point is the starting point q1. According to the above method, the traced connection points are sequentially added to the boundary pixel set. Finally, the algorithm creates a vector-based residential polygon based on the recorded coordinates of the boundary pixels.

1) EXTRACTION OF STARTING BOUNDARY POINT

Because the endpoint of the hatched line is in the interior of the boundary polygon of the residential area, a 45-degree ray that passes through the endpoint of the hatched line must be

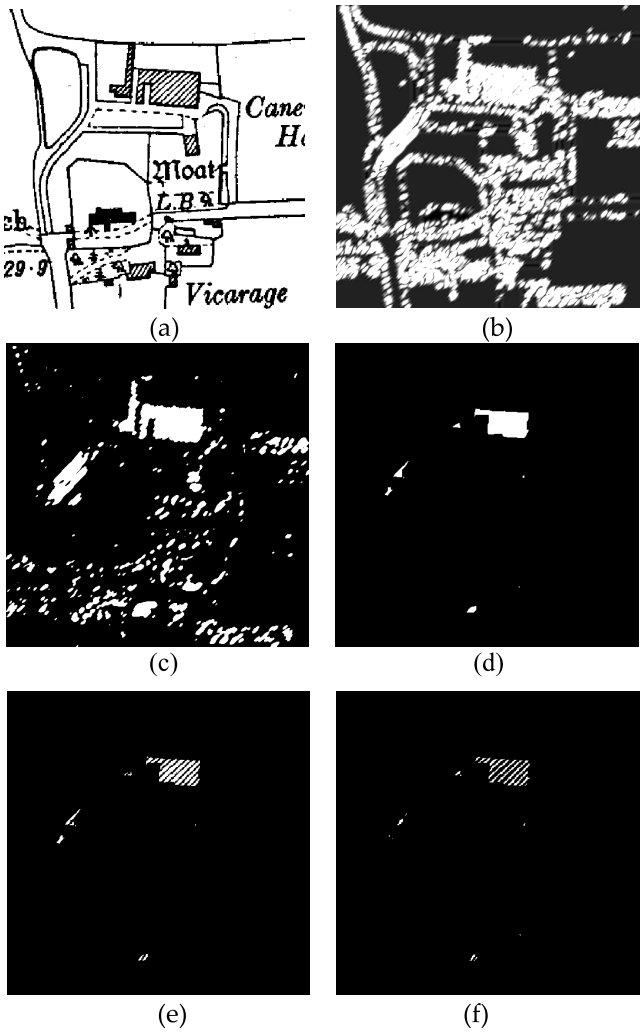

FIGURE 10. Detection of hatched lines in map 1: (a) the binary original image, (b) the filtering result of Gabor filter, (c) the result of Gaussian smoothing and binarization, (d) the result of erosion, (e) the clipped hatched line image, (f) the hatched line image represented with white.

intersected with the external boundary of the residential area. Based on the known endpoint p0 of the hatched line, firstly, we calculate the pixel q0 that has the same coordinate with p0 in the original binary image. Then starting from the pixel q0 and taking a pixel as the step length to search black pixels along the northeast 45 degrees direction. If the found pixel is white, considering connection directions of some adjacent pixels in the boundary of the hatched line are not always 45 degrees. Now we need to judge whether the white pixel within the residential area or not so as to distinguish the tracking point whether arrives in the boundary of residential area. Here we adopt dynamic filling strategy to judge: with the white pixel as the seed point, the white area connected to it is filled with black, if the area of the filled area is less than or equal to the threshold value Ts (Ts is estimated by artificial observation, which is the maximum value of the white area surrounded by two adjacent hatched lines and the boundary of the residential area in an image), it shows the white pixel in internal of residential area. After filling the white connection area using black, we take the white pixel location as the new starting point and regard a pixel as step length, and continue to search for black pixels along the northeast 45 degrees direction until we find a white pixel which connecting white area is greater than the threshold Ts. Assuming the coordinate of the white point pixel found at the end is (x, y), and its pixel value is denoted as q(x, y). Let the tracking point goes back a step length along the previous tracking direction, then the tracking point in the new location is a residential area boundary point, which coordinate is (x-1, y+1), but if q (x-1, y) = 0 (black) and q (x, y+1) = 0 (black), in this case, in order to improve the speed of tracking boundary points, the pixel (x-1, y) can be directly set as the starting point for tracking boundary.

2) THE METHOD OF TRACKING BOUNDARY POINTS

After calculating the tracking starting point q1 of the residential area boundary, to track the boundary points in the original binary image. The steps and methods of tracking the boundary point of residential areas are as follows: Let the coordinate of pixel q1 is (x, y), and the pixel value of q1 is p (x, y) = 0 (black). Starting from q1 (q1 is the initial tracking point). Our algorithm searches a pixel (i, j) that is one of the eight adjacent pixels and meets the conditions of formulas (5-6) at the same time as the tracking connecting point q2.

$$p(i,j) = 0 \tag{5}$$

$$\begin{aligned} p(i-1,j) &= 1 orp(i+1,j) = 1 orp(i,j-1) \\ &= 1 orp(i,j+1) = 1 \end{aligned} \tag{6}$$

Then, we trace the boundary point connecting with q2. Following the above method to keep tracking the next boundary point until the first starting boundary point is traced. If the residential area boundary line only has two pixels width, it is needed to judge whether the connection point is the inner point of the boundary or the outer point (by judging the area size of white connecting regions that connects with the connecting point. Ts is the threshold), and keep the outer point as the tracking connection point. If the found connection point is a bulgy pixel, such as the C pixel in Figure 5, the pixel should be regarded as a noise that to be removed. After removing the noise, using the previous tracking point to track the connection point again.

For the adhesions like roads or other objects connecting with the boundary of residential area, this paper designs a bar-shaped detector to detect the adhesion objects. The principle is to calculate the number of black pixels that the bar-shaped detector intersects with the binary original image to determine whether the intersecting pixels belong an adhesive object. If they are the adhesive noises, our algorithm will deal with them as follows. As shown in Figure 6, there are eight kinds of spatial position relationships between two adjacent points on the boundary (the connection point C and the previous connection point P).

TABLE 1. Experimental parameters and results (N is the maximum width (pixel number) of the part where the adhesive object connects the residential area).

Map	Image size: height (pixel) *width (pixel)	N (pixel)	Length of the bar-shaped detector (pixel)	Ts: Threshold of the filled area (pixel)	Times of eroding Gabor area	Identification rate (%)
1	512*512	6	10	400	6	100%
2	256*256	7	10	200	4	100%
3	512*512	6	10	400	7	83.3%

A line segment with single pixel width starting at point C and perpendicular to the PC is called a bar-shaped detector. The line segment including n pixels may be on the left of $\overrightarrow{PC}$ or on the right of $\overrightarrow{PC}$, as shown in Figure 7.

In the detection process, starting from the point C, the pixel values of the backup binary image are sequentially inquired along the bar-shaped detector at the corresponding pixel location. If the queried pixel is black, the number of intersecting black pixels increases by 1. If the queried pixel is white, taking the pixel as the seed point and filling the connecting white area with black. If the area is less than or equal to a certain threshold Ts (it indicates that the filled area is a blank area inside the residential area), filling the original binary image of the residential area, the number of intersecting black pixels increases by 1. If the last accumulated number of black pixels is greater than the threshold value N (it is the customized noise size, which is defined as the maximum width (pixel number) of the part where the adhesive object connects the residential area), our algorithm keeps the point C as the connection point. If the filled area is greater than the threshold Ts (it indicates that the filled area is a blank area outside the residential area), moreover the counted number of black pixels is less than or equal to N, starting from the point C our algorithm sequentially wipes off the black pixels one by one in the original binary image along the forward direction of the strip detector until the scanned pixel is a white pixel. The main purpose of such treatment is to cut off the other ground objects connecting with the residential area. Finally our algorithm uses P to find the new connection point again. If encountering a pixel that has been a boundary point in the detection process (such a situation usually occurs at the corner of the polygon of the residential area), it is not necessary to erase black pixels along the stripe detector, and this moment C is judged as the boundary point.

IV. EXPERIMENT, RESULT ANALYSIS AND DATA FUSION

To demonstrate the effectiveness and practicability of our proposed method, we developed a program for algorithm implementation and experiments, as shown in Figure 8. The experimental platform adopted the Microsoft Visual Studio. Net 2013 integrated development platform, and developed program with C#.NET, ArcGIS Engine10.2, EmguCV and Aforge.Net. The experimental computer hardware configuration is of Intel (R) Core (TM) i7-6500U processor, 16GB memory and 1000GB storage space.

We selected three typical residential areas images from historical raster maps as the experimental data (Figure 9). The data of Figure 9a is from the National Library of Scotland website (https://maps.nls.uk/view/101457131). Its map scale is six inches to one statute mile and its publication date is 1924. The data of Figure 9b is 1:50000 scale topographic map (sample map, the second edition in 1979, the map number is J-49-135-C, in 1979) from the website (http://ngcc.sbsm.gov.cn/article/sjcg/dtxz/e/) of National Geographic Information Center in China. The data of Figure 9c is from literature [7] (the map scale is 1:50000). The data quality of the above experimental datasets are poor, for example, fuzzy boundary of residential area, irregular arrangement of boundary pixels, symbol adhesion. The boundary identification result of experimental data in Figure 9 is given in Figure 10 (Figure 10a is the result of Figure 9a, Figure 10b is the result of Figure 9b, Figure 10c is the result of Figure 9c). Table 1 shows the experimental parameters and results of test data in Figure 9. Where the identification rate is equal to the ratio of the number of polygons identified by our algorithm to the number of the hatched residential areas that people think the computer could identify. We set the values of experimental parameters according to data analysis and multiple experiments.

In our experiments, the relevant parameters in Gabor formula were $\gamma = 0.5$, $\lambda = 4$, $\theta = \pi/4$, $\sigma = 2.24$ (according to formula (4), taking the bandwidth b= 1, in the meantime $\sigma = 0.56 * \lambda$) and $\varphi = 0$. To accurately locate the position of residential area, the Gabor area was needed to be shrunk properly using erosion operations to ensure it was situated within the residential area. The image erosion used 3×3 filter mask.

Figure 10 shows the detection process of hatched lines in map 1. Figure 10a is the binary image of map1 (Figure 9a). Figure 10b is the filtering result of Figure 10a using the Gabor filter. Figure 10c is the result of carrying Gaussian smoothing and binarization of Figure 10b in sequence. Figure 10d is the result of carrying six erosion operations of Figure 10c. Figure 10e is the result of and-operation of Figure 10d and Figure 10a, which is the hatched line image that is cut out

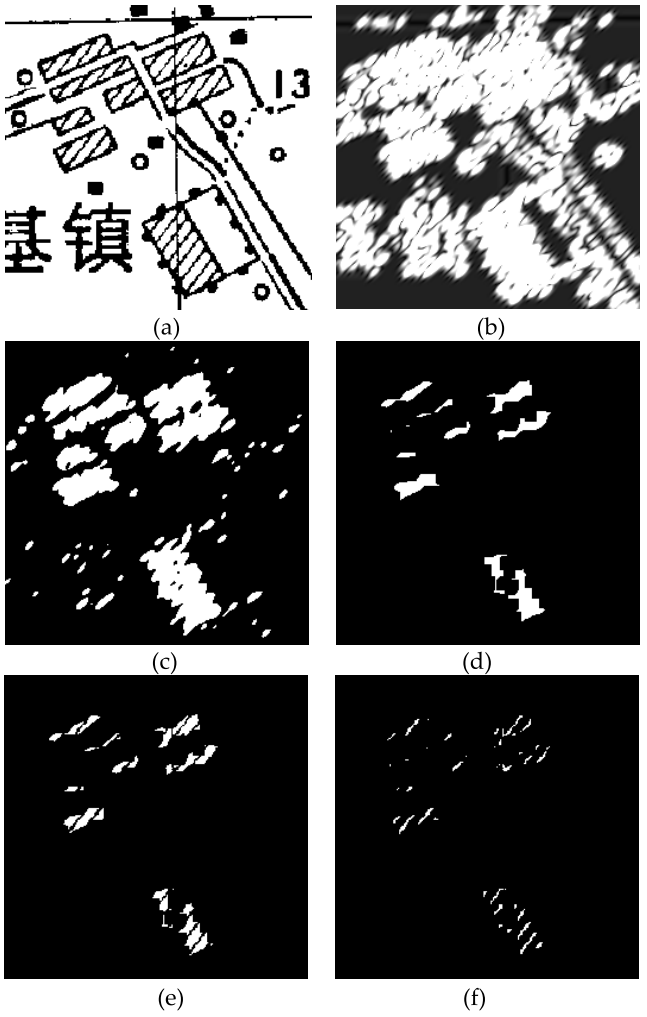

FIGURE 11. Detection of hatched lines in map 2: (a) the binary original image, (b) the filtering result of Gabor filter, (c) the result of Gaussian smoothing and binarization, (d) the result of erosion, (e) the clipped hatched line image, (f) the hatched line image represented with white.

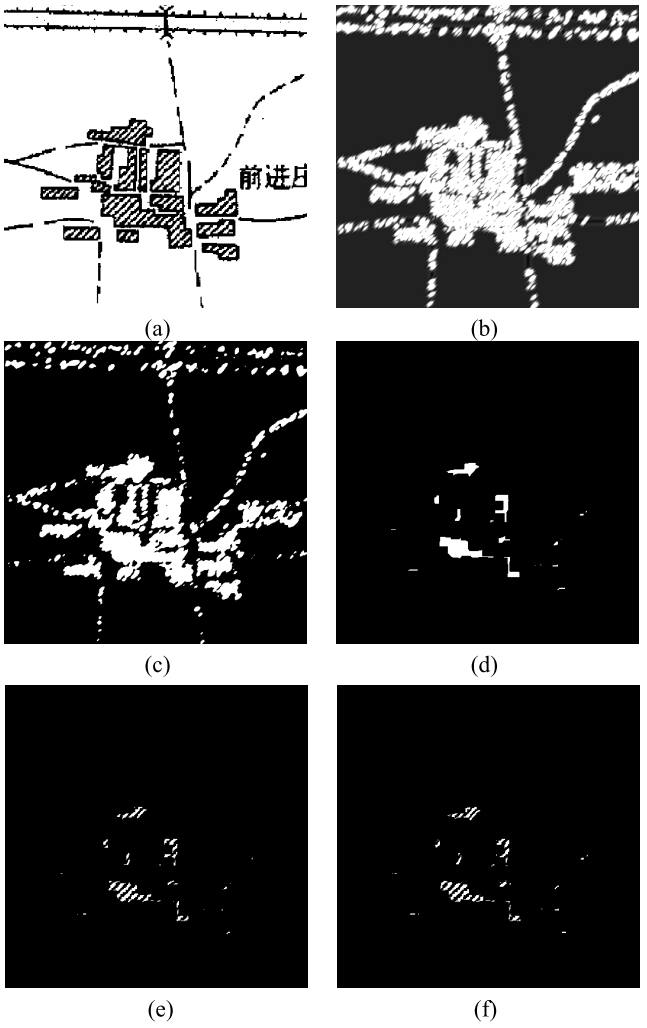

FIGURE 12. Detection of hatched lines in map 3: (a) the binary original image, (b) the filtering result of Gabor filter, (c) the result of Gaussian smoothing and binarization, (d) the result of erosion, (e) the clipped hatched line image, (f) the hatched line image represented with white.

from the binary original image. Figure 10f is the result of subtraction operation of Figure 10d and Figure 10e, which is the hatched line image where hatched lines denoted in white.

Figure 11 shows the detection process of hatched lines in map 1. Figure 11a is the binary image of map 2 (Figure 9b). Figure 11b is the filtering result of Figure 11a using the Gabor filter. Figure 11c is the result of carrying Gaussian smoothing and binarization of Figure 11b in sequence. Figure 11d is the result of carrying four erosion operations of Figure 11c. Figure 11e is the result of and-operation of Figure 11d and Figure 11a, which is the hatched line image that is cut out from the binary original image. Figure 11f is the result of subtraction operation of Figure 11d and Figure 11e, which is the hatched line image where hatched lines denoted in white.

Figure 12 shows the detection process of hatched lines in map 3. Figure 12a is the binary image of map 3 (Figure 9c). Figure 12b is the filtering result of Figure 12a using the Gabor filter. Figure 12c is the result of carrying Gaussian smoothing and binarization of Figure 12b in sequence. Figure 12d is the result of carrying seven erosion operations of Figure 12c. Figure 12e is the result of and-operation of Figure 12d and Figure 12a, which is the hatched line image that is cut out from the binary original image. Figure 12f is the result of subtraction operation of Figure 12d and Figure 12e, which is the hatched line image where hatched lines denoted in white.

As shown in Figure 9, the method proposed in this paper could identify residential areas with hatched lines, and that it could effectively identify the hatched residential areas that are adhered by road or other elements. Besides the identification of boundary line was the outer contour line of the residential areas polygons. The overall effect was good, and achieved the expected effect. However, it was difficult to identify the residential areas of relatively small area (area≤around 400 pixels) or where the number of internal hatched lines less than three (just as the residential areas within red circle in Figure 9a, which human also think are unrecognizable).

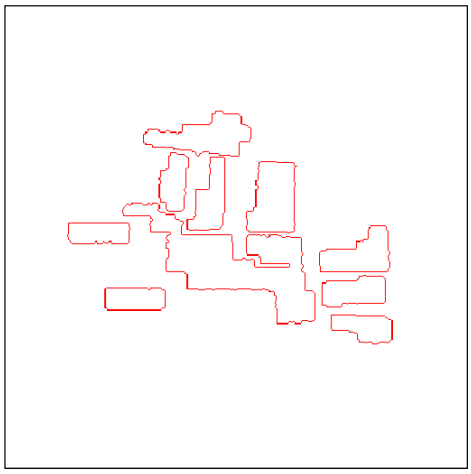

(a)

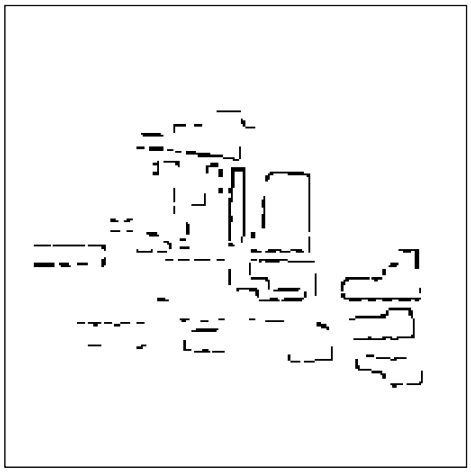

(b)

FIGURE 13. Comparison of experiment results: (a) The identification result of this paper; (b) The identification result of literature [7].

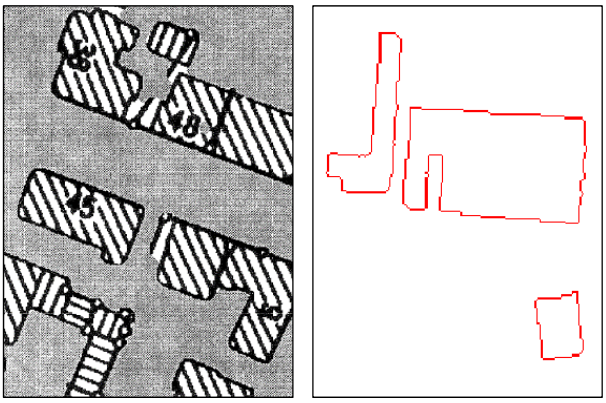

(a) (b)

FIGURE 14. Comparison of experiment results: (a) Final result of literature [9]; (b) Residential area boundary extracted by this paper.

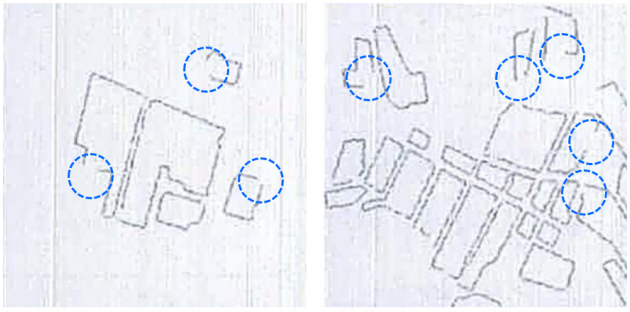

FIGURE 15. Initial contour extracting results literature [12].

The main reason was that the hatched line could not be detected. Besides, sometimes the bar detector could cause the corner of residential area polygons to become smooth (sometimes it would wrongly take some pixels on corner as noises). In addition, this paper compared and analyzed the experimental results.

(1) For the map 3 in Figure 9, we compared our proposed method with the residential area identification method based on structural feature in literature [7]. Figure 13 clearly demonstrates that the identified boundaries (Figure 13a) of our method have the advantages of complete boundary and high position accuracy in comparison to the identification result of literature [7]) (Figure 13b). In Figure 13b, the line thickness of identified boundaries is different, which indicates the positional accuracy of the boundary is uncertain, however the boundary lines extracted by this paper are from outlines of original residential area graphics and their line thickness is one pixel. Moreover, the process of the proposed method in literature [7] is complicated because it requires the image processing operations including four-direction RLS transformation, intersection and union, shrinking, expanding, refining and so on.

(2) Comparing our method with the method of the literature [9]. As shown in Figure 14, we found that literature [9] roughly extracted the regional range of the residential area, instead of accurately extracting the residential boundaries. But our method extracted clearer and more accurate residential boundaries.

(3) Comparing our method with the method of the literature [12]. Although both of them used Gabor filter to detect hatched residential area, but the literature [12] required for the hatched line to conduct refining operation in the boundary extraction process in order to track the starting point of the contour tracking. Refining could lead to fractured and incomplete hatched lines, and the uncertain position of starting tracking point. In addition, it stopped tracking when encountering adhesive symbols, so it needed to connect the fracture contour line in the late. Two initial contour extracting results of literature [12] are shown in Figure 15. We may find many fractured boundaries indicated by the blue circle in Figure 16.

Furthermore, the connection of the adjacent endpoints of the disconnected location depended on the manual setting of the spatial search scope. And that it required the hatched line

(a)

(b)

FIGURE 16. Application of data fusion: (a) Integrating the extracted residential areas with Google aerial image, (b) Integrating the extracted residential areas with Google map.

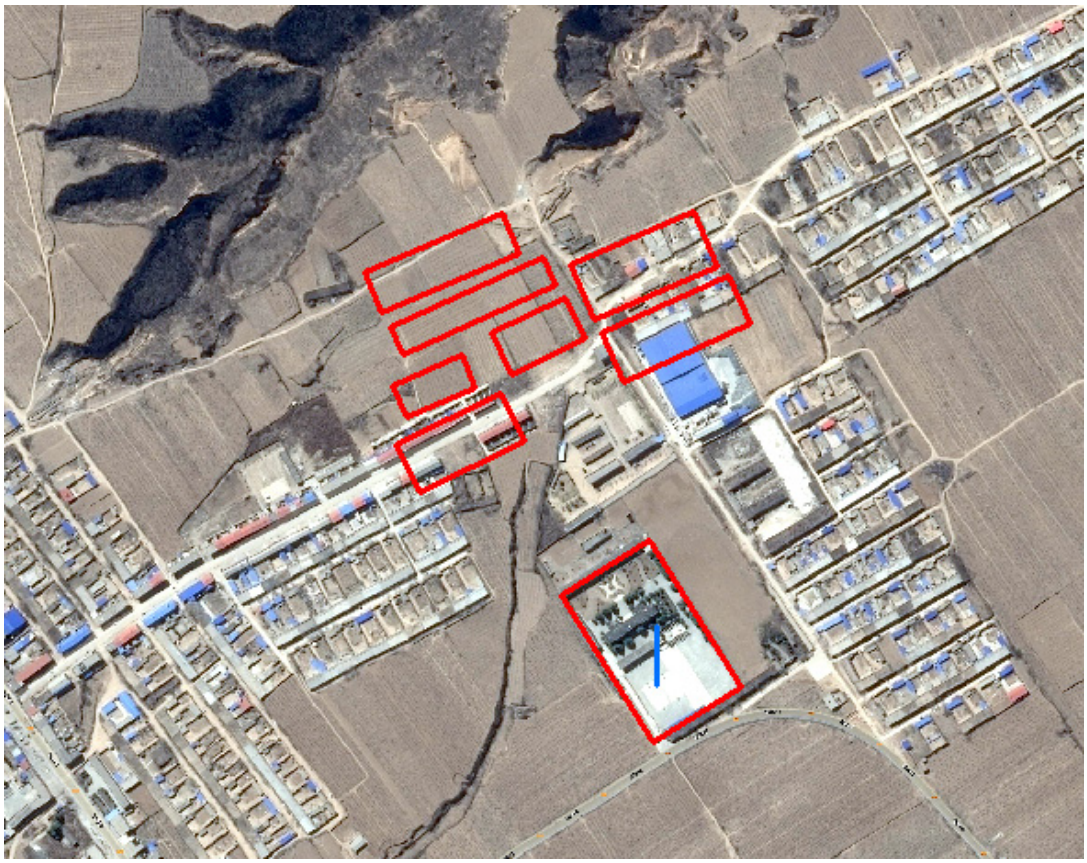

FIGURE 17. Data fusion of the identified result data of map 2 and aerial image.

to be detected must be connected with the contour line. But the algorithm and strategy proposed by this paper overcome the above problems. We can obtain the closed boundaries of residential areas in most cases (as shown in Figure 9(d-f)).

Furthermore, we generated the ArcGIS-formatted vector data by using the coordinate values stored in the coordinate text file. And the extracted polygons of the residential areas were processed by coordinate transformation, map projection information configuration, vertex rarefying and right-angle by ArcMap (for example, using ''generalize'' tool in Advance Editing toolbar for vertex rarefying) and some manual processing. In the process we vectorized the St Nicholas Church so that the map from different sources could be matched, because the church hasn't changed much. Then we integrated the processed vector polygon data with aerial image and map from Google Maps website. Figure 16 shows the data fusion results. Where the red polygons are residential areas and the St Nicholas Church. The blue lines connect the possible identical entities from different data sources. Due to the different cartographic methods, it is difficult for identical entities from different data sources to overlap completely even if spatial adjustment is made. From Figure 16 we can know the distribution of residential areas in the region in the 1920s or before, and it is easy to see that great changes took place in the region from the 1920s to 2018.

Analogously we modified the identified result data of map 2 in Figure 9b and integrated it with aerial image from Google Maps website. As shown in Figure 17. We may find that great changes took place in this region except for one residential area.

For map 3 in Figure 9c, possibly because of great changes in topography and semantics, and lack of geographical coordinate information, we cannot find accurate matching region for map 3. Therefore, the data fusion does not be realized.

V. CONCLUSIONS

This paper proposed a new Gabor filter-based method for automatic recognition of hatched residential areas. The validity and practicability of the method are verified by experiments involving three typical data from Scotland and China. Compared with previous methods, our method has some advantages of high automation degree of extraction (e.g., when users input a color image and set several parameters, the identified result image can be generated after clicking the graphic recognition menu shown in Figure 8), complete boundary, high position accuracy of boundary and high anti-noise performance. In general, our method is suitable for extracting the contour of the residential area with parallel hatched lines toward northeast 45 degrees direction from a scanned raster topographic map, not suitable for building

extracting from remote sensing image. It can be easily used for extracting residential areas with parallel hatched lines toward other direction by adjusting algorithm parameter, and it performs better for the raster map with high resolution (For example, the image resolution is over 200dpi).

Moreover, our method also has disadvantages, such as it depends on parameter setting, requires the close boundary of residential area and cannot directly extract residential areas from a complete map sheet. For these shortcomings, we need to improve it in the future research work, to further improve the adaptability and effectiveness of the method by increasing the number of experimental cases and the range of experimental areas. And it has the limitation of cannot extracting the boundary of residential area with less than three parallel hatched lines or with blurry filling texture. Besides, the automated methods of rarefying, smoothing and rectangularity processing of vector boundary are still to be studied in the next step. The proposed method in this paper is beneficial for the application analysis of historical raster topographic maps and multi-source geographic information fusion, for example, integrating the paper map and RS imagery, or integrating the paper map and vector spatial data.

REFERENCES

[1] J. H. Uhl, S. Leyk, Y. Y. Chiang, W. W. Duan, and C. A. Knoblock, "Map archive mining: Visual-analytical approaches to explore large historical map collections," *Int. J. Geo-Inf.*, vol. 7, no. 4, p. 148, 2018.

[2] Y. Y. Chiang, S. Leyk, and C. A. Knoblock, "Efficient and robust graphics recognition from historical maps," in *Proc. Int. Conf. Graph. Recognit., New Trends Challenges*, in Lecture Notes in Computer Science, vol. 7423, Y.-B. Kwon and J.-M. Ogier, Eds. Berlin, Germany: Springer-Verlag, 2013, pp. 25–35.

[3] S. Spinello and P. Guitton, "Contour line recognition from scanned topographic maps," *J. WSCG*, vol. 12, nos. 1–3, pp. 419–426, 2004.

[4] Y. Y. Chiang, C. A. Knoblock, C. Shahabi, and C. C. Chen, "Automatic and accurate extraction of road intersections from raster maps," *Geoinformatica*, vol. 13, no. 2, pp. 121–157, 2009.

[5] S. Leyk and R. Boesch, "Extracting composite cartographic area features in low-quality maps," *Cartogr. Geograph. Inf. Sci.*, vol. 36, no. 1, pp. 71–79, 2009.

[6] X. Liu, Z. X. Zhang, J. Q. Zhang, and J. N. Huang, "Automatic recognition of houses in large-scaled topographic maps," *Chin. J. Comput.*, vol. 21, no. 11, pp. 1027–1032, 1998.

[7] X. Y. Hao, Z. W. Lu, C. B. Wu, and Q. Xi, "The recognition of hatched polygons based on structural characteristics," *J. PLA Inst. Surv. Mapping*, vol. 16, no. 1, pp. 27–32, 1999.

[8] H.-L. Zheng, X.-Z. Zhou, and H.-B. Wang, "Automatic extraction and recognition of elements in topographic maps based on morphological decomposition," *MINIMICRO Syst.*, vol. 25, no. 6, pp. 1072–1075, 2004.

[9] R. Brfigelmann, "Recognition of hatched cartographic patterns," *Int. Arch. Photogramm. Remote Sens.*, vol. 31, no. 3, pp. 82–86, 1996.

[10] Z. L. Fu, *Automatic Recognition Technology of Scanned Map Image*. Beijing, China: Surveying Mapping Press, 2003, pp. 1–20.

[11] S. Y. Hu, C. Zhi, and Y. Zhou, "Recognition system for residential areas in maps," *J. SHANGHAI JIAOTONG Univ.*, vol. 32, no. 9, pp. 90–92, 1998.

[12] Y. Chen, Z. P. Fu, R. S. Wang, and J. Zhang, "Automatic recognition of hatched residential areas in color scanned topographical maps," *J. Comput.-Aided Des. Comput. Graph.*, vol. 20, no. 11, pp. 1459–1465, 2008.

[13] Y. Yang, C. Q. Zhu, and Q. Sun, "Extraction and vectorization of street blocks on scanned topographic maps," *Sci. Surv. Mapping*, vol. 32, no. 5, pp. 88–90, 2007.

[14] D. Gabor, "Theory of communication. Part 1: The analysis of information," *J. Inst. Elect. Eng. Jpn.*, vol. 93, no. 26, pp. 429–441, 1946.

[15] J. G. Daugman, "Uncertainty relation for resolution in space, spatial frequency, and orientation optimized by two-dimensional visual cortical filters," *J. Opt. Soc. Amer. A, Opt. Image Sci.*, vol. 2, no. 7, pp. 1160–1169, 1985.

[16] R. Kong and B. Zhang, "Design of Gabor filters' parameter," *Control Decis.*, vol. 27, no. 8, pp. 1277–1280, 2012.

[17] I. Sertcelik, O. Kafadar, and C. Kurtulus, "Use of the two dimensional Gabor filter to interpret magnetic data over the Marmara Sea, Turkey," *Pure Appl. Geophys.*, vol. 170, no. 5, pp. 887–894, 2013.

[18] H. L. Yang, J. Yuan, D. Lunga, M. Laverdiere, A. Rose, and B. Bhaduri, "Building extraction at scale using convolutional neural network: Mapping of the United States," *IEEE J. Sel. Topics Appl. Earth Observ. Remote Sens.*, vol. 11, no. 8, pp. 2600–2614, Aug. 2018.

[19] R. Alshehhi, P. R. Marpu, W. L. Woon, and M. D. Mura, "Simultaneous extraction of roads and buildings in remote sensing imagery with convolutional neural networks," *ISPRS J. Photogramm. Remote Sens.*, vol. 130, pp. 139–149, Aug. 2017.

[20] J. H. Uhl, S. Leyk, Y. Y. Chiang, W. W. Duan, and C. A. Knoblock, "Extracting human settlement footprint from historical topographic map series using context-based machine learning," in *Proc. 8th Int. Conf. Pattern Recognit. Syst. (ICPRS)*, Madrid, Spain, 2017, pp. 1–6.

JIANHUA WU received the Ph.D. degree in photogrammetry and remote sensing from Wuhan University, in 2008. Moreover, he was a Visiting Scholar with the Spatial Sciences Institute, University of Southern California (2015–2016). He is currently an Associate Professor with the School of Geography and Environment, Jiangxi Normal University. His current research interests include intelligent perception and service of geospatial information, geospatial data matching and integration, geographic information systems, and graphics recognition. He has ever participated in and hosted numerous GIS projects (two projects granted by the National Natural Science Foundation of China).

PENGJIE WEI is currently pursuing the Ph.D. degree in cartography and geographical information systems. Her current research interests include graphic recognition, social media data mining, and geographic information engineering.

XIAOFANG YUAN is currently pursuing the Ph.D. degree in cartography and geographical information systems. Her current research interests include spatio-temporal information extraction from social media data and geographic information engineering.

ZHIGANG SHU received the master's degree in cartography and geographical information systems from the School of Geography and Environment, Jiangxi Normal University, in 2017. His current research interests include graphic recognition and land information systems.

YAO-YI CHIANG received the Ph.D. degree in computer science from the University of Southern California, in 2010. He is currently an Associate Professor with the Spatial Sciences Institute, University of Southern California. He has published a number of articles on automatic techniques for geospatial data extraction and integration. His general areas of research are artificial intelligence and data science, with a focus on information integration and spatial data analytics. He develops computer algorithms and applications that discover, collect, fuse, and analyze data from heterogeneous sources to solve real world problems. He is also an expert on digital map processing and geospatial information system (GIS).

ZHONGLIANG FU received the Ph.D. degree in photogrammetry and remote sensing from Wuhan Technical University of Surveying and Mapping (now it is Wuhan University), in 1996, where he is currently a Professor and a Doctoral Supervisor with the School of Remote Sensing and Information Engineering. His current research interests include geospatial data management and update, geospatial data matching and integration, remote sensing image processing, and geographic big data mining.

MIN DENG received the Ph.D. degree from Wuhan University, in 2003, and the Asian Institute of Technology, in 2004. He is currently a Professor and also a Doctoral Supervisor with the School of Geosciences and Info-Physics, Central South University. His current research interests include geospatial data update, spatio-temporal data mining, and spatio-temporal analysis and modeling.